Journal of Alloys and Compounds, 186 (1992) 77–87
JALCOM 258

CVD of Y_2O_3 from YCl_3–CO_2–H_2–Ar gas mixtures: an experimental study

E. Sipp, F. Langlais and R. Naslain
Laboratoire des Composites Thermostructuraux (UMR47, CNRS-SEP-UB1), Domaine Universitaire, 3 allée de la Boëtic, F-33600 Pessac (France)

(Received December 27, 1991)

Abstract

The chemical vapor deposition of Y_2O_3 from YCl_3–CO_2–H_2–Ar gas mixtures is studied in a graphite hot-wall deposition chamber. YCl_3 gas flows are generated by vaporization of liquid YCl_3 in an argon stream and controlled by recording *in situ* the mass loss of the YCl_3 graphite crucible with a millibalance. The deposits are performed on alumina substrates and the Y_2O_3-deposition rates are assessed *in situ* with a microbalance. When $[CO_2]_{in}/[YCl_3]_{in} > 9$, the deposits consist of pure Y_2O_3; otherwise YOCl is the main deposited phase. At $P = 4$ kPa, the deposition process is rate controlled by surface reactions for $T < 1100$ °C and $500 < Q_{tot} < 1000$ sccm, whereas beyond these limits mass transfers across the boundary layer become the rate-limiting phenomena. When controlled by surface reactions, the Y_2O_3 deposition process is thermally activated with $E_a = 616$ kJ mol^{-1}, $k_0 = 4.4 \cdot 10^{11}$ $mg \cdot min^{-1} \cdot cm^{-2} \cdot Pa^{-5}$ and the apparent partial reaction orders are $n_1 = 2$; $n_2 = 2$; $n_3 = 1$ and $n_4 = 0$ with respect to YCl_3, H_2, CO_2 and HCl.

Introduction

Yttria is commonly used to stabilize zirconia in its tetragonal or cubic forms. It also exhibits specific properties that might justify its use, as a pure phase, for structural applications at high temperatures. The melting point of yttria, 2410–2415 °C [1, 2], is intermediate between those of alumina (2050 °C) and zirconia (≈2700 °C). Yttria is also one of the most stable refractory oxides [3, 4]. It could be used, associated with carbon, up to about 2050 °C, *i.e.* at a service temperature as high as that of zirconia [5]. The density of yttria, $d = 5.0$ $g \cdot cm^{-3}$, is much higher than those of covalent ceramics (*e.g.* 3.27 $g \cdot cm^{-3}$ for SiC) but could still be acceptable for specific structural applications. Another important advantage of yttria (with respect to zirconia) is that it crystallizes as a single modification (cubic cell with $a = 1.06$–1.0604 nm; crystal structure related to that of CaF_2), that is stable from room temperature to the melting point [1]. Y_2O_3 is a white phase when it is stoichiometric, whereas it is black when it has been heated at high temperatures under a reducing atmosphere [6].

Several authors have studied the mechanical properties of Y_2O_3 and the effect of deviations from stoichiometry on its mechanical behavior. According to Fantozzi and Orange [6], the toughness K_{IC} of stoichiometric Y_2O_3 is 3.5

0925-8388/92/$5.00

$MPa \cdot m^{1/2}$, whereas it is only 2.3 $MPa \cdot m^{1/2}$ for non-stoichiometric yttria. In a similar manner, the fracture energy values are respectively 57 $J \cdot m^{-2}$ and 24.5 $J \cdot m^{-2}$ for stoichiometric and non-stoichiometric yttrias. Finally, they have shown that the hardness does not depend on the chemical composition ($H_V = 7.4$ and 7.7 GPa for stoichiometric and non-stoichiometric yttria). This feature has also been reported by Tsukuda [7].

Despite the intrinsic properties of Y_2O_3, the thermostructural applications of yttria have remained rather limited up to now, possibly as a result of the high cost of rare earth element compounds. Tsukuda has shown that yttria pipes remain undamaged after an ageing treatment of 100 h in air at 2100 °C whereas (i) MgO and Al_2O_3 pipes broke when aged at 1950 °C for 6 h and 2 h respectively and (ii) zirconia pipes aged at 1950 °C for 100 h did not fail but cracked on cooling and therefore could not be used a second time [2].

As far as we know, the chemical vapor deposition (CVD) of yttria has never been studied in a detailed manner. However, some information on the CVD of yttria has been available within the frame of studies devoted to mixed oxides involving Y_2O_3. The first mentions of the CVD of yttria were in studies devoted to the deposition of YIG by Binachon [8] and of $Re_3Fe_5O_{12}$ (with Re ≡ Y, Gd) by Kleinert and Kirchof [9]. Further data on the CVD of yttria can be found in studies relating to the deposition of Y_2O_3-stabilized zirconias [11, 12, 18]. More recently, the research on Y_2O_3-based superconducting complex oxides (*e.g.* YBaCuO) gave a new interest to the CVD of Y_2O_3 [10, 22]. Different gaseous precursors of yttrium have been suggested, the most often used being YCl_3 [8, 9] or yttrium organometallic compounds such as 2,2,6,6-tetramethylheptadionate-(3,5)Y, ($Y(thd)_3$) which has the advantage of being stable up to 200–250 °C and non-hygroscopic [11–13].

The aim of the present contribution was to derive the kinetic law corresponding to the CVD of pure Y_2O_3 from YCl_3–CO_2–H_2–Ar mixtures from an experimental study with a view to exploring the potential of CVD–Y_2O_3 (either as pure Y_2O_3 or Y_2O_3-stabilized zirconias) as a component in ceramic matrix composites.

2. Experimental details

The CVD of Y_2O_3 from a gaseous YCl_3–CO_2–H_2–Ar mixture is thought to result from the hydrolysis of YCl_3 by water formed *in situ* by the hydrogen reduction of CO_2 at high temperatures; according to the following overall chemical mechanism (which is similar to those already suggested for the deposition of both alumina and zirconia) [14, 15]:

$$3H_2(g) + 3CO_2(g) \rightleftharpoons 3H_2O(g) + 3CO(g) \quad (1)$$

$$2YCl_3(g) + 3H_2O(g) \rightleftharpoons Y_2O_3(s) + 6HCl(g) \quad (2)$$

or by combining eqns. (1) and (2):

$$2YCl_3(g) + 3H_2(g) + 3CO_2(g) \rightleftharpoons Y_2O_3(s) + 3CO(g) + 6HCl(g) \quad (3)$$

2.1. CVD apparatus

The CVD unit used to deposit Y_2O_3 films from YCl_3–CO_2–H_2–Ar mixtures is shown schematically in Fig. 1. Gaseous YCl_3 is obtained by vaporizing liquid YCl_3 (Aldrich (ref. 29, 826-3)) heated in a graphite crucible (diameter 30 mm, height 155 mm) with an r.f. coil and a graphite susceptor. The YCl_3 vapor is transported to the deposition chamber with a flow of argon. The CVD experiments were performed in a hot-wall low pressure deposition chamber consisting of a graphite tube (diameter 68 mm, thickness 4 mm, height 350 mm) heated with an r.f. coil and a graphite susceptor. Hydrogen and CO_2 were mixed at room temperature; the mixture was then preheated by passing it across the hot YCl_3(g) generator and finally admitted to the CVD chamber. It has been calculated that the deposition substrate has to be located about 30 mm below the hot gas inlet in order to ensure a laminar flow.

The temperatures of the deposition chamber and YCl_3(g) generator were measured with B-type Pt/Rh and K-type chromel–alumel thermocouples respectively. The flow rates were measured with mass gas flow-meters (ASM) for all the common species (*i.e.* argon, hydrogen and CO_2). Conversely, that of gaseous YCl_3 was measured according to a specifically designed procedure as follows: (i) the graphite crucible containing the YCl_3 source was attached to an electronic millibalance (type PM400, Mettler), (ii) the mass of vaporized YCl_3 was continuously recorded *versus* time and (iii) the YCl_3 gas flow rate

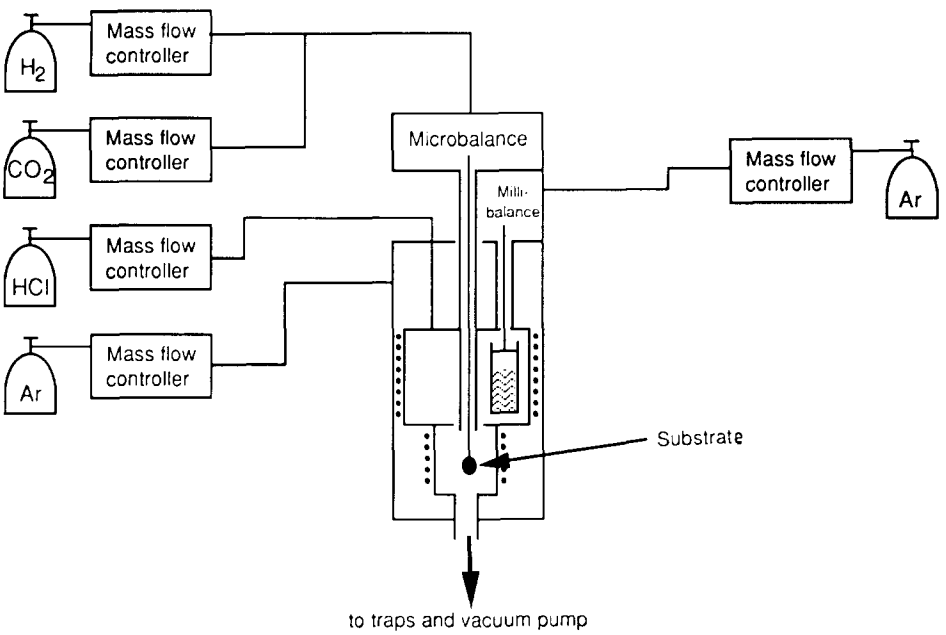

Fig. 1. Apparatus used for the CVD of Y_2O_3 (schematic).

was calculated from the crucible mass loss according to the following equation:

$$Q_{YCl3}(\text{sccm}) = 22\,400 \cdot 60 \cdot \frac{1}{M_{YCl3}} \cdot \frac{\Delta m}{\Delta t} \quad (4)$$

where M_{YCl3} is the molar mass of YCl_3 in grams and $\Delta m/\Delta t$ is the vaporization rate of YCl_3 ($g \cdot s^{-1}$) (*i.e.* the slope of $\Delta m = f(\Delta t)$ is a straight line when steady state is achieved). More details about the measurement of YCl_3 gas flow rate have been reported elsewhere [16].

The total pressure was maintained constant with a pressure-controlling device (252A from MKS Instruments) at a given value within the range 0.1–13 kPa. The CVD experiments were performed at temperatures ranging from 1000 to 1300 °C, the isothermal zone being of the order of 50 mm ($\Delta T \pm 6$ °C). Deposition occurred on an alumina substrate consisting of cylindrical pellets (diameter 10 mm, thickness 1 mm) (Al_2O_3 from Degussa) attached with a tungsten wire to a microbalance (B85 from Setaram). Under such conditions, the amount of Y_2O_3 deposited on the alumina substrate could be recorded continuously as a function of time with a relative accuracy of the order of 10^{-6} g (in fact a mass variation of $2.5 \cdot 10^{-6}$ g could easily be detected).

2.2. Deposit characterization

The Y_2O_3 CVD films were characterized by X-ray diffraction (XRD with a filtered Cu Kα radiation diffractometer Philips PW 1050) and scanning electron microscopy (JEOL JSM-840-A).

3. Results and discussion

3.1. Nature of the deposit

CVD experiments were performed with gaseous YCl_3–CO_2–H_2–Ar mixtures corresponding to various $[CO_2]_{in}$:$[YCl_3]_{in}$ ratios, on alumina substrates. As shown in Fig. 2, the deposit consists of yttrium oxychloride YOCl (mixed with trace amounts of Y_2O_3) for $[CO_2]_{in}$:$[YCl_3]_{in} = 4$ (Fig. 2(a)) whereas it is made of pure Y_2O_3 for $[CO_2]_{in}$:$[YCl_3]_{in} = 9$ (Fig. 2(b)).

This result is in full agreement with the conclusions of a thermodynamic study of the deposits obtained from the complex $ZrCl_4$–YCl_3–CO_2–H_2–Ar system reported by Sipp *et al.* [17]. According to these authors, solid YOCl is formed instead of Y_2O_3 when the initial gas composition is poor in CO_2.

As shown in Fig. 3, the Y_2O_3 deposits (obtained for $T = 1090$ °C and $P = 4$ kPa) consist of well-facetted irregular platelet-like crystals, the mean size of which is of the order 10 μm. These crystals are apparently randomly orientated in the deposits.

3.2. Effect of the CVD parameters on the deposition rate

3.2.1. Temperature

The thermal variations of the deposition rate R, of Y_2O_3, are shown in Fig. 4 as Arrhenius plots for two different values of the total pressure (*i.e.* $P = 2$ and 4 kPa).

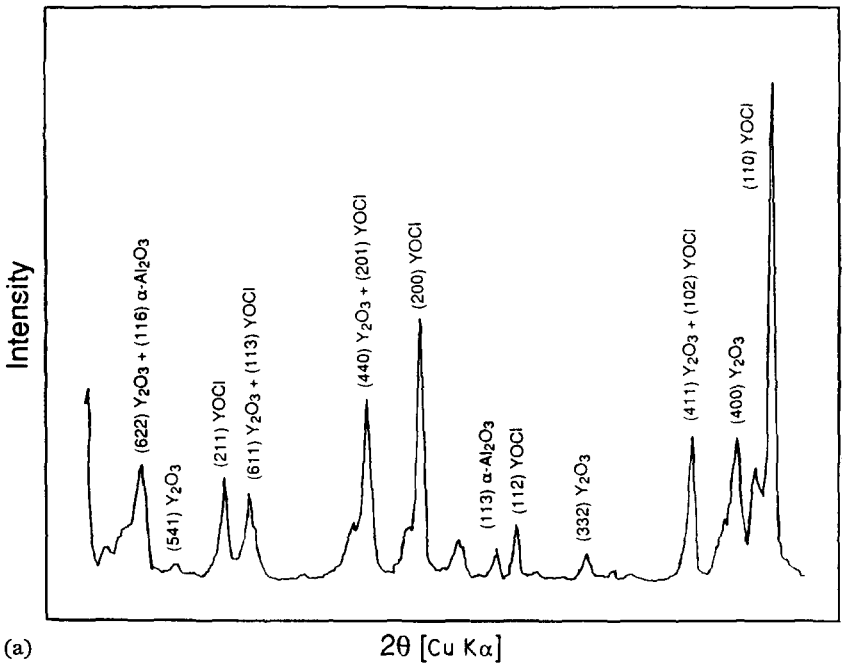

(a)

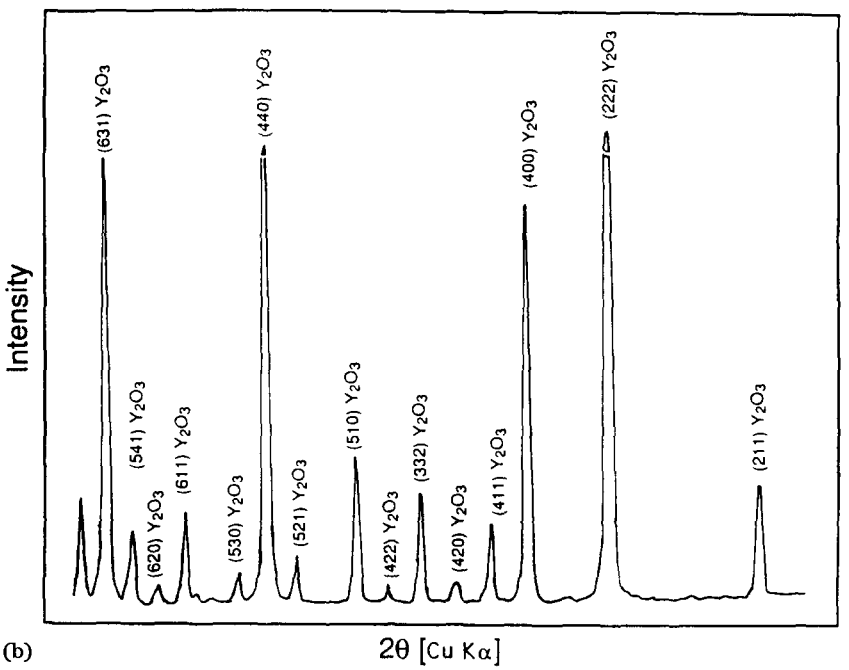

(b)

Fig. 2. Debye–Sherrer patterns of Y_2O_3 deposited from YCl_3–H_2–CO_2–Ar on an alumina substrate: (a) $T = 1090$ °C, $P = 4$ kPa, $Q_{H_2} = 120$ sccm, $Q_{CO_2} = 40$ sccm, $Q_{YCl_3} = 4.5$ sccm, $Q_{Ar} = 460$ sccm; (b) $T = 1090$ °C, $P = 4$ kPa, $Q_{H_2} = 60$ sccm, $Q_{CO_2} = 20$ sccm, $Q_{YCl_3} = 4.5$ sccm, $Q_{Ar} = 460$ sccm.

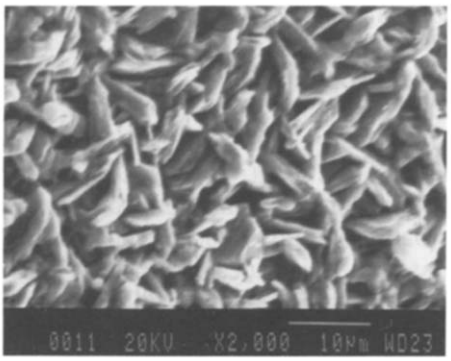

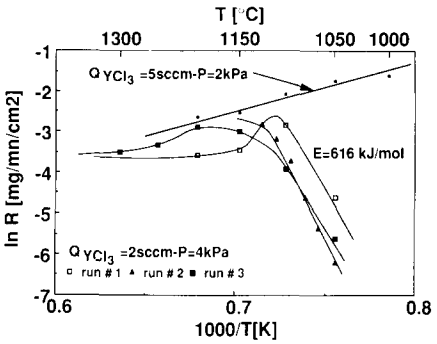

Fig. 3. Scanning electron micrograph of an Y_2O_3-deposit obtained at $T=1090$ °C and $P=4$ kPa.

Fig. 4. Arrhenius plots of the thermal variations of the yttria deposition rate for two pressures ($Q_{H_2}=60$ sccm, $Q_{CO_2}=20$ sccm, $Q_{Ar}=260$ sccm).

At low pressures (*i.e.* for $P=2$ kPa), the deposition process does not seem to be thermally activated within the whole temperature range studied. In fact, the deposition rate slowly decreases in a continuous manner as the temperature is increased from 1000 °C, a feature that suggests that the deposition kinetics might already be controlled by mass transfer across the boundary layer even at this rather low temperature.

At higher pressures (*i.e.* $P=4$ kPa), the data can be discussed on the basis of a more classical scheme. At low temperatures (*i.e.* $T<1100$ °C), the deposition process appears to be thermally activated, as supported by the occurrence of linear relationships between $\ln R$ and $1/T$. The related apparent activation energies are respectively 514; 538 and 765 kJ·mol^{-1}, with a mean value of 616 kJ·mol^{-1}. This value is not too far from that reported previously by Wahl *et al.* [18] (*i.e.* 406 kJ·mol^{-1}). At high temperatures (*i.e.* $T>1100$ °C), the deposition rate tends towards a limit, a feature that suggests that the deposition kinetics might be limited by mass transfer across the boundary layer. It is worthy of note that this limit is similar to that achieved at high temperatures for $P=$ 2kPa.

3.2.2. Total pressure

The variations of the Y_2O_3 deposition rate as a function of the total pressure are shown in Fig. 5 for $T=1100$ °C and 1250 °C. Generally speaking, the deposition rate is high at low pressures (*i.e.* $P<1$ kPa), then decreases sharply as pressure is raised, and finally tends towards a limit (which is roughly the same for the two temperatures). At a given low pressure, *e.g.* $P=2$ kPa, the deposition rate is higher for $T=1100$ °C than for $T=1250$ °C, in agreement with the data shown in Fig. 4. On the basis of the data shown in Figs. 4 and 5, it seems that the transition between a deposition process rate controlled by mass transfers and a process limited by surface

reaction kinetics induced by a pressure variation might occur for a pressure close to 2 kPa.

Finally, the general features of the variations of the deposition rate of Y_2O_3 (from YCl_3–CO_2–H_2–Ar), as a function of pressure, are somewhat similar to those previously reported for SiC (from CH_3SiCl_3–H_2) [19], BN (from BF_3–NH_3) [20] and ZrO_2 (from $ZrCl_4$–CO_2–H_2–Ar) [15].

3.2.3. Total gas flow rate

The effect of the total gas flow rate on the deposition rate depends on the dimensions of the CVD chamber. However, the flow rate has to be studied to define the conditions under which the deposition kinetics are controlled by surface reactions. Since the CVD experiments reported in this section were performed at constant temperature, total pressure and chemical composition of the feed gas, any variation of the deposition rate Q as a function of the total gas flow rate Q_{tot} has to be related to hydrodynamic effects and not to chemical effects.

The effects of Q_{tot} on R is shown in Fig. 6. At a rather high total pressure (*i.e.* $P=4$ kPa), the deposition rate first increases rather sharply when Q_{tot} is raised from 300 to 500 sccm; it then remains constant (for 500–900 sccm) and finally increases again (for $Q_{tot}>900$ sccm). Under this condition, increasing the temperature from 1100 °C to 1250 °C results in a simple translation of the deposition rate towards higher values. At a lower total pressure (*i.e.* $P=2$ kPa), the $R=f(Q_{tot})$ curve exhibits the same general features as obtained for $P=4$ kPa. However, the transition between the first two parts of the curve is less pronounced.

The occurrence of a plateau in $R=f(Q_{tot})$ suggests that within the corresponding Q_{tot} range the deposition kinetics might be controlled by surface chemical reactions and not by mass transfers in the boundary layer. The transition between both regimes as Q_{tot} is increased is clearly apparent for $P=4$ kPa, in agreement with the Arrhenius plots shown in Fig. 4. Conversely, it is much less apparent and even questionable for $P=2$ kPa.

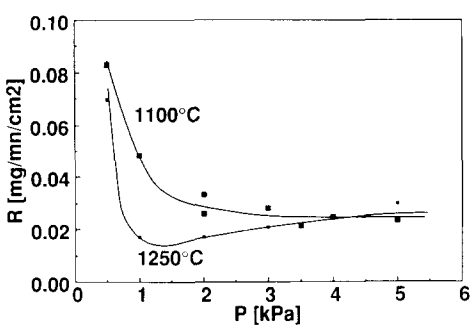

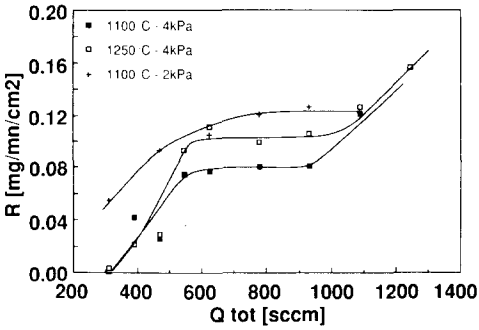

Fig. 5. Variations of the yttria deposition rate as a function of the total pressure ($Q_{H_2}=60$ sccm, $Q_{CO_2}=20$ sccm, $Q_{YCl_3}=2$ sccm, $Q_{Ar}=260$ sccm).

Fig. 6. Variations of the yttria deposition rate as a function of the total flow rate ($X_{H_2}=0.193$ kPa, $X_{CO_2}=0.064$ kPa, $X_{YCl_3}=0.003$ kPa, $X_{Ar}=0.740$ kPa).

3.3. Effect of the partial pressures on the deposition rate: partial apparent reaction orders

The CVD experiments reported in Section 3.2. have shown that the deposition process of Y_2O_3 is rate limited by the surface reactions under the following conditions: $T<1100$ °C, $P\approx 4$ kPa and Q_{tot} ranging from 500 to 1000 sccm. These conditions were selected to establish the kinetic law corresponding to Y_2O_3 deposition from YCl_3–CO_2–H_2–Ar, through the study of the effect of the partial pressures of the various species (reactants and products) on the deposition rate.

For a species i, the experiments were performed by maintaining constant flow rates Q_j and partial pressures P_j of all the species j (with $j\neq i$) and by varying the total pressure and the partial pressure P_i of the species i under consideration. The data are shown in Figs. 7–10 as $\ln R=f(\ln P_i)$ curves. These curves are expected to be straight lines, slopes of which are the

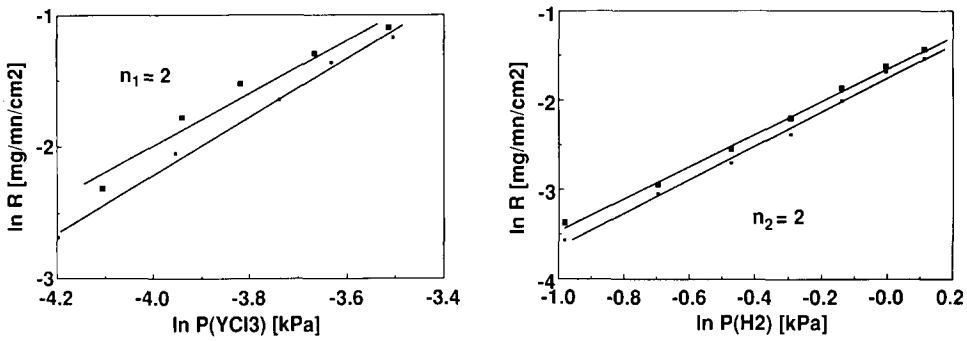

Fig. 7. Variations of the deposition rate of yttria as a function of the YCl_3 partial pressure ($P_{H_2}=0.771$ kPa, $P_{CO_2}=0.257$ kPa, $P_{Ar}=2.955$ kPa, $T=1090$ °C).

Fig. 8. Variations of the deposition rate of yttria as a function of the H_2 partial pressure ($P_{CO_2}=0.374$ kPa, $P_{YCl_3}=0.025$ kPa, $P_{Ar}=3.227$ kPa, $T=1090$ °C).

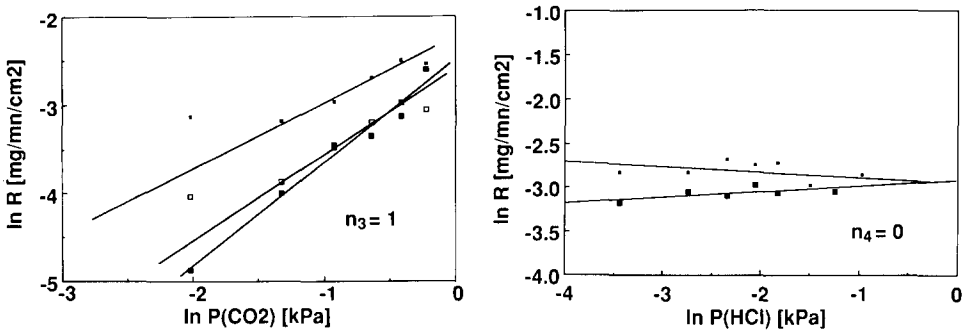

Fig. 9. Variations of the deposition rate of yttria as a function of the CO_2 partial pressure ($P_{H_2}=0.399$ kPa, $P_{YCl_3}=0.027$ kPa, $P_{Ar}=3.342$ kPa, $T=1090$ °C).

Fig. 10. Variations of the deposition rate of yttria as a function of the HCl partial pressure ($P_{H_2}=0.772$ kPa, $P_{CO_2}=0.257$ kPa, $P_{YCl_3}=0.013$ kPa, $P_{Ar}=2.958$ kPa, $T=1090$ °C.

apparent reaction orders, in agreement with a kinetic law of the following kind:

$$R = k_0 \exp\left(-\frac{E_a}{\mathbf{R}T}\right) \cdot P_{YCl_3}^{n_1} \cdot P_{H_2}^{n_2} \cdot P_{CO_2}^{n_3} \cdot P_{HCl}^{n_4} \quad (5)$$

where k_0 is the pre-exponential surface kinetics constant, E_a the apparent activation energy, **R** the perfect gas constant and n_1, n_2, n_3, n_4 the apparent partial reaction orders with respect to the reactants (YCl_3, H_2, CO_2) and product (HCl).

3.3.1. Partial reaction orders with respect to reactants

From the data shown in Figs. 7–9, the apparent partial reaction orders with respect to the reactant species are $n_1 = 2$ for YCl_3, $n_2 = 2$ for hydrogen and $n_3 = 1$ for CO_2.

3.3.2. Partial reaction order with respect to HCl

In a CVD process, it is sometimes of interest to study the effect on the deposition rate of adding increasing amounts of a reaction product to the feed gas, *e.g.* HCl in the deposition of Y_2O_3 from YCl_3–H_2–CO_2–Ar gas mixtures (see eqns. (2) and (3)).

The reaction orders n_4 that have been calculated from the data shown in Fig. 10 are respectively $n_4 = 0.06$ and -0.07 for the two series of experiments considered here. Therefore, it was assumed that the apparent partial reaction order with respect to HCl is $n_4 = 0$, a feature that means that the addition of HCl to the feed gas has no effect on the deposition rate of Y_2O_3 under the experimental conditions mentioned above.

It is worthy of note that HCl is added to the feed gas, in the deposition of YIG from $FeCl_3$–YCl_3–O_2, in order to avoid nucleation phenomena in the gas phase [21]. This result, when compared with our data, suggests that the chemical oxidation mechanism of the metal chlorides might be different, depending on whether the oxidizing species is molecular oxygen or water vapor.

3.4. Kinetics law

From the data reported in Sections 3.1., 3.2. and 3.3., the following kinetics law is proposed:

$$R = k_0 \exp\left(-\frac{E_a}{\mathbf{R}T}\right) \cdot P_{YCl_3}^{2} \cdot P_{H_2}^{2} \cdot P_{CO_2}^{1} \cdot P_{HCl}^{0} \quad (6)$$

where R is expressed in $mg \cdot min^{-1} \cdot cm^{-2}$, $k_0 = 4.4 \cdot 10^{11}\ mg \cdot min^{-1} \cdot cm^{-2} \cdot Pa^{-5}$ and $E_a = 616\ kJ \cdot mol^{-1}$. It should be emphasized that this law is valid only for the experimental conditions $T < 1100$ °C, $P \approx 4$ kPa, $500 < Q_{tot} < 1000$ sccm and for the specified partial pressures already mentioned.

4. Conclusion

From the experimental data reported in the present contribution on the CVD of Y_2O_3 from YCl_3–CO_2–H_2–Ar gas mixtures, the following conclusions can be drawn.

(1) When the amount of the oxidizing source species CO_2 is high enough (*i.e.* $[CO_2]_{in}:[YCl_3]_{in} > 9$), the deposit consists of pure Y_2O_3 (conversely, YOCl becomes the main component when this condition is not fulfilled).

(2) At a high enough total pressure (*e.g.* 4 kPa), the Y_2O_3 deposition process is rate controlled by surface reactions as long as the temperature remains lower than about 1100 °C and the total gas flow rate falls within the range 500–1000 sccm. Beyond these limits, mass transfers across the boundary layer become the rate-controlling phenomena.

(3) In the surface reaction controlled regime, the deposition process of Y_2O_3 is thermally activated with an apparent activation energy of 616 $kJ \cdot mol^{-1}$ and a pre-exponential kinetics constant of $k_0 = 4.4 \cdot 10^{11}$ $mg \cdot min^{-1} \cdot cm^{-2} \cdot Pa^{-5}$.

(4) Under the rather narrow experimental conditions studied here, the kinetics law can be written as:

$$R = k_0 \exp\left(-\frac{E_a}{RT}\right) \cdot P_{YCl_3}^2 \cdot P_{H_2}^2 \cdot P_{CO_2}^1 \cdot P_{HCl}^0$$

Acknowledgments

This work has been supported by Société Européenne de Propulsion (through a grant given to E.S.) and CNRS. The authors are indebted to C. Robin-Brosse (from SEP) for fruitful discussions on various experimental aspects.

References

1 Pascal, Traité de Chimie Minérale – Eléments des Terres Rares, 778.
2 Y. Tsukuda, Application of yttria as refractory material, *J. Can. Ceram. Soc.*, *52* (1983) 14–17.
3 W. D. Kingery, *Property measurements at high temperatures*, Wiley, New York, 1959.
4 W. D. Kingery, High Temperature Technology, *Proc. Int. Symp., Asilomar, CA*, McGraw-Hill, New York, 1960.
5 J. L. Pentecost, in J. Huminik, Jr., (ed.), *High Temperature Inorganic Coatings*, Reinhold, New York, 1963, p. 10.
6 G. Fantozzi and G. Orange, *J. Am. Ceram. Soc.*, *72* (8) (1989) 1562–63.
7 Y. Tsukuda, *Mater. Res. Bull.*, *16* (1981) 453–459.
8 J. C. M. Binachon, *Thesis*, Université Grenoble, Grenoble, 1973.
9 P. Kleinert and J. Kirchhof, *Z. anorg. allg. Chem.*, *429* (1977) 147–155.
10 H. Suhr, Ch. Oehr, H. Holszschuh, F. Schmaderer, G. Wahl, Th. Kruck and A. Kinnen, *Physica C, 153–155* (1988) 784–785.

11 K. Kamata, S. Matsumoto and Y. Shibata, *Yogyo-Kyokai-Shi, 90/1* (1982) 46–47.
12 K. Brennfleck, E. Fitzer and G. Schoch, in J. O. Carlsson and J. Lindström (eds.), *Proc. 5th European CVD Conf.*, Uppsala University Press, Uppsala, 1985, pp 63–70.
13 J. P. Dismukes, J. Kane, B. Binggęli and H. P. Schweizer, Chemical vapor deposition of cathodoluminescent phosphor layers, in G. F. Wakefield and J. M. Blocher, Jr., (eds.), *Proc. 4th Int. Conf. CVD*, The Electrochemical Society Inc., Boston, MA, 1973, pp. 275–282.
14 R. Colmet and R. Naslain, *Wear, 80* (1982) 221–231.
15 J. Minet, F. Langlais and R. Naslain, *J. Less-Common Met., 132* (1987) 273–287.
16 E. Sipp, F. Langlais and C. Bernard, to be published.
17 E. Sipp, F. Langlais, R. Naslain and C. Bernard, to be published.
18 G. Wahl, S. Schlosser and F. Schmaderer, in T. O. Sedgwick and H. Lydtin (eds.), *Proc. 7th Int. CVD Conf.*, Los Angeles, CA, The Electrochemical Society, Boston, MA, 1979, pp. 536–548.
19 F. Langais and C. Prébendé, in K. E. Spear and G. W. Cullin (eds.), *Proc. 11th Int. Conf. on CVD*, The Electrochemical Society, Pennington (1990) 686.
20 T. Matsuda, H. Wakae and T. Hirai, *J. Mater. Sci., 28* (1988) 509.
21 M. Mikami and K. Matsumi, *J. Cryst. Growth, 37* (1977) 1–8.
22 L. V. Interrante, Z. Jiang and D. J. Larkin, in D. L. Nelson and T. F. George (eds.), *Chemistry of High-Temperature Superconductors II*, American Ceramic Society Symposium Series 377, Columbus, OH, (1988) 168–180.